

1           **Surface salinity under transitioning ice cover in the**  
2           **Canada Basin: Climate model biases linked to vertical**  
3           **distribution of freshwater**

4           **E. Rosenblum<sup>1</sup>, R. Fajber<sup>2</sup>, J. C. Stroeve<sup>1,3,4</sup>, S. T. Gille<sup>5</sup>, L. B. Tremblay<sup>6</sup>, E.**  
5           **C. Carmack<sup>7</sup>**

6           <sup>1</sup>Centre for Earth Observation Science, University of Manitoba, Winnipeg, Manitoba, Canada.

7           <sup>2</sup>University of Washington, Seattle, Washington, USA

8           <sup>3</sup>Centre for Polar Observation and Modelling, University College London, Earth Sciences, London, United  
9           Kingdom

10          <sup>4</sup>National Snow and Ice Data Center, Cooperative Institute for Research in Environmental Sciences,  
11          University of Colorado, Boulder, CO, USA

12          <sup>5</sup>Scripps Institution of Oceanography, University of California San Diego, La Jolla, California, USA

13          <sup>6</sup>Department of Atmospheric Science, McGill University, Montreal, Quebec, Canada

14          <sup>7</sup>Fisheries and Oceans Canada, Sidney, British Columbia, Canada

15           **Key Points:**

- 16           • Community Earth Systems Model versions 1.1 and 2 significantly underestimate  
17           decadal surface freshening in the Canada Basin.
- 18           • The surface freshening model bias is likely not related to seasonal freshwater in-  
19           put at the surface from sea ice melt or other sources.
- 20           • The models distribute freshwater over an unrealistically large depth range in re-  
21           cent years, which contributes to the surface salinity bias.

---

Corresponding author: =name=, =email address=

## Abstract

The Canada Basin has exhibited a significant trend toward a fresher surface layer and thus a more stratified upper ocean over the past three decades. Here, we explore the extent to which the Community Earth System Model (CESM) accurately simulates the observed surface freshening and seasonal processes that contribute to the freshening. We examine 30 simulations from CESM1 (used in the IPCC AR5), 3 simulations from CESM2 (IPCC AR6), and ocean observations from 1975 and 2006-2012. In contrast to the observations, the models simulate salinity profiles that show relatively little variation between 1975 and 2012. We demonstrate that this bias can be partly attributed to the model's tendency to mix freshwater too deep, creating a surface layer that is saltier than observed. The results provide insight for climate model improvement that could have wide-reaching implications because upper-ocean stratification influences the vertical transport of heat and nutrients.

## Plain Language Summary

Climate models, which have been analyzed extensively to assess and predict current and future climate change and to inform policy, struggle to accurately simulate the rapid decline in Arctic sea ice. One possible source of this bias could be related to the vertical distribution of salt in the ocean, which controls the exchange of heat between the surface and deeper ocean. We compare simulations from two climate models to ocean observations collected below sea ice in the Canada Basin. In 1975, observations were collected by scientists living in ice camps, and in 2006-2012, they were obtained by automated instruments attached to sea ice. The observations indicate as much as six times greater surface freshening than the models between 1975 and 2006-2012. We show that the salt bias can be partly attributed to the models' tendency to mix freshwater from the surface deeper than in observations, resulting in a saltier ocean surface. The results may provide insight for climate model improvement that could have wide-reaching implications because the vertical distribution of salt in the ocean directly impacts the vertical transport of heat and nutrients.

## 1 Introduction

Rapid sea ice retreat has been extensively observed in the Canada Basin over the past several decades (F. McLaughlin et al., 2011). The increased sea ice melt and river runoff that have collected toward the center of the anticyclonic (convergent) Beaufort Gyre (Proshutinsky et al., 2009; Yamamoto-Kawai et al., 2009; F. A. McLaughlin & Carmack, 2010; E. C. Carmack et al., 2016; Wang et al., 2018; Brown et al., 2020) drive a 30-year 1.1-1.9 psu/yr trend toward a fresher surface layer (Peralta-Ferriz & Woodgate, 2015). The addition of this relatively light, freshwater at the surface has stabilized the upper ocean, altering ice-ocean processes, including wind-driven mixing, the vertical transport of heat and nutrients, and sea ice basal melt (Toole et al., 2010; Jackson et al., 2010, 2011, 2012; Steele et al., 2011; E. Carmack et al., 2015; M. L. Timmermans, 2015; M. Timmermans & Marshall, 2020).

Historically, climate models simulate a slower sea ice retreat than observed (Stroeve et al., 2007; Winton, 2011; Stroeve et al., 2012; Rosenblum & Eisenman, 2016, 2017; SIMIP, 2020). One possible source of the model bias could be related to simulated upper-ocean stratification, which tends to be less stratified than in observations (Holloway et al., 2007; Ilicak et al., 2016). The ocean stratification bias could be related to unrealistic sea ice conditions, which could result in too little freshwater input from sea ice melt each season. Alternatively, the biases could be related to unrealistic ocean processes, such as vertical diffusion (Zhang & Steele, 2007) or brine rejection schemes (Nguyen et al., 2009). Up until now, this problem has mainly been investigated with numerical experiments or by comparing simulations to annual climatologies with little to no attention paid to their

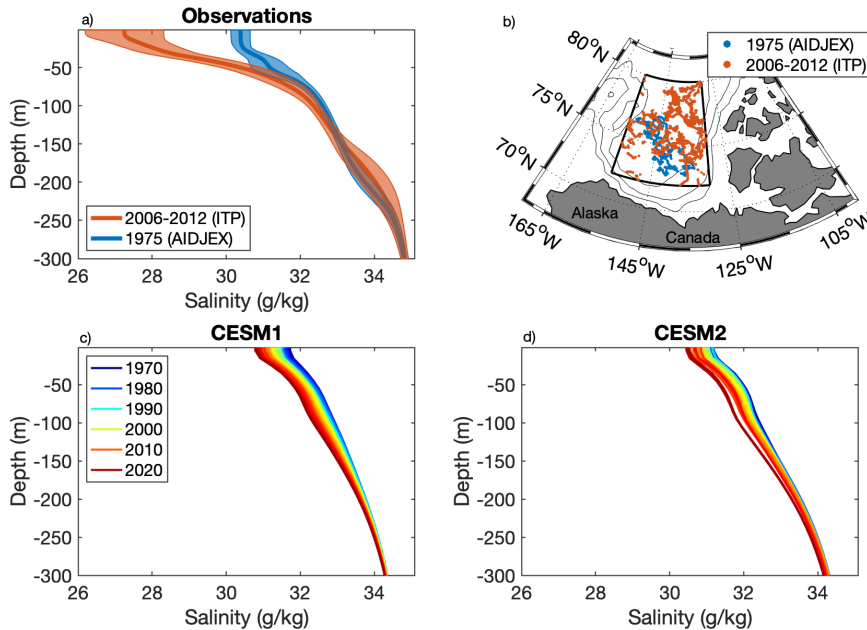


**Figure 1.** Observed salinity profiles from 1975 AIDJEX data (blue) and 2006-2012 ITP data (red). Solid line indicates May-December average and shading indicates one standard deviation. (b) Map showing the Canada Basin, the locations of 1975 AIDJEX data (blue) and 2006-2012 ITP data (red), and the region considered for this study (black lines). (c-d) Simulated May-December ensemble-mean basin average salinity profiles in 1970-2020 from (c) CESM1 and (d) CESM2.

72 seasonality (Holloway et al., 2007; Ilicak et al., 2016; Nguyen et al., 2009; Zhang & Steele,  
73 2007; Jin et al., 2012; Barthélemy et al., 2015; Sidorenko et al., 2018).

74 Here, we explore this problem by examining both sea ice conditions and ocean pro-  
75 cesses in models and observations using simulations from the two most recent genera-  
76 tions of the Community Earth System Model (CESM1 and CESM2), both of which are  
77 extensively used in polar studies and in the Intergovernmental Panel on Climate Change  
78 (IPCC) Fifth and Sixth Assessment Reports (AR5 and AR6), and two sets of year-round  
79 ocean observations collected in the Canada Basin during 1975 and 2006-2012. Our main  
80 objective is to understand what governs the seasonal salinity evolution in the models and  
81 observations in the Canada Basin by examining seasonal surface processes related to sea  
82 ice conditions, freshwater input, and vertical mixing, all of which cumulatively contribute  
83 to decadal surface freshening. Distinguishing between atmospheric and oceanic processes  
84 that cause surface freshening in the models and observations is critical for determining  
85 if model freshening mechanisms are consistent with the natural world and helps to iden-  
86 tify processes that might be missing or poorly simulated in the models.

## 87 2 Methods

88 We use year-round below-ice observations of ocean salinity collected in the Canada  
89 Basin, defined as the region enclosed by 72°N, 80°N, 130°W, and 155°W (Fig. 1b), from  
90 the 1975 Arctic Ice Dynamics Joint Experiment (AIDJEX) program (Untersteiner et al.,  
91 2007) and during 2004-present from the Ice-Tethered Profiler (ITP) instrumen-  
92 tation system (Krishfield et al., 2008). There were four occupied AIDJEX ice camps between May

1975 and April 1976 and 30 ITPs, which were available for 2004-2012 at the time of the analysis. The data in this study are identical to those employed by Rosenblum et al. (2021), who showed that June-September surface changes between the ITP and AIDJEX datasets are consistent with 30-year mixed-layer trends reported by Peralta-Ferriz and Woodgate (2015) in the same region. They used only quality-controlled data (level 3) in the ITP archive, screened profiles to select those that include samples above 10 m depth (as in Jackson et al., 2010) and that were collected during the period May 1 - December 31, which is common to both datasets. In total, 754 AIDJEX profiles during 1975 and 3391 ITP profiles during 2006-2012 from 12 ITPs (#1, 3-6, 8, 11, 13, 18, 33, 41, and 53) satisfied these criteria, with average shallowest measurements of  $\sim 6$  m and  $\sim 7$  m, respectively (Fig 1b). Profiles were linearly interpolated onto a common 1 m vertical grid, and the shallowest values were extended to  $z = 0$ , which we take as the ice-ocean interface, as in the models.

To examine sea ice conditions associated with the ITP dataset, we identify co-located daily sea ice concentrations, provided by the Passive Microwave satellite data, Version 1 (Cavalieri et al., 1996). Weekly, regional-mean sea ice concentrations associated with the AIDJEX data are provided by the Canadian Ice Service Digital Archive (CISDA) chart data for the western Arctic region (Tivy et al., 2011). We also examine estimates of the 1979-2018 effective sea ice thickness (sea ice volume per unit area) from the Pan Arctic Ice Ocean Modeling and Assimilation System (PIOMAS) (Schweiger et al., 2011). PIOMAS effective sea ice thickness was regridded to the 25km Equal-Area Scalable Earth (EASE) grid, and data were collected from each grid cell residing in the Canada Basin. While several studies have shown that PIOMAS tends to underestimate sea ice thickness in regions of thicker ice and overestimate sea ice thickness in regions of thinner ice (Stroeve et al., 2014; Wang et al., 2018), the seasonality, spatial structure, distribution, and decadal trends of the sea ice thickness are realistically reproduced (Labe et al., 2018).

We use 30 simulations of 1970-2020 from CESM1 with historical and RCP8.5 forcing from the Large Ensemble project (Kay et al., 2015) and three simulations from CESM2 with historical and SSP585 forcing. CESM1 and CESM2 are run with historical forcing until 2005 and 2015, respectively. Both models use the Parallel Ocean Program Version 2 (POP2) model with a displaced pole horizontal grid, a nominal  $1^\circ$  resolution, 60 vertical levels, and 10 m vertical grid spacing near the surface, although some of the physical parameterizations, including the K-profile parameterization (KPP) vertical ocean mixing scheme (Large et al., 1994), differ between the two models (Danabasoglu et al., 2020). We examine the ocean salinity, the effective sea ice thickness, the sea ice concentration in each grid box within the Canada Basin of each simulation (Table S1).

## 3 Results

### 3.1 Upper-ocean salinity

The May-December average ocean salinity over the top 300 m in the models and the observations is shown in Figure 1. The observations indicate a significantly fresher upper-ocean over the top 50 m in 2006-2012 than in 1975, with the largest differences occurring at the surface (Fig. 1a), consistent with previous studies. By contrast, the 1970-2020 ensemble mean only shows only a modest freshening from the surface down to 200 m in both models (Fig. 1c-d). This results in a simulated upper-ocean stratification that is weaker than in recent observations, similar to other ice-ocean models.

To eliminate the possibility that regional or internal variability could explain the bias, we examine the surface salinity from each observation and each grid point of each simulation during each month (Figure 2). In each dataset, we find a clear seasonal cycle where the surface becomes fresher in the summer and saltier in the fall, coinciding with seasonal sea ice evolution. In each month, we find that the models systematically

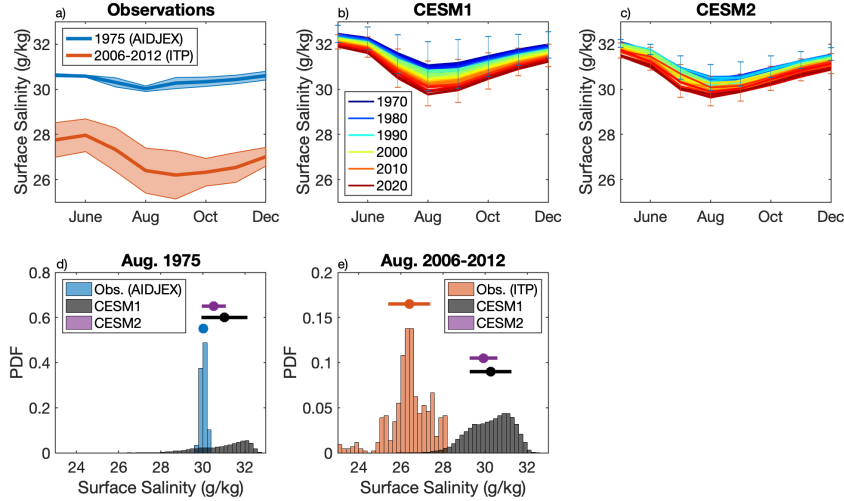


**Figure 2.** (a) Surface salinity from 1975 AIDJEX data (blue) and 2006-2012 ITP data (red). Solid line indicates May-December average and shading indicates standard deviation. Blue and red error bars indicate one standard deviation over all grid points and simulations in 1975 and 2006-2012, respectively. (b-c) Simulated 1970-2020 ensemble-mean surface salinity from (b) CESM1 and (c) CESM2. Distribution of August surface salinity in (d) 1975 and (e) 2006-2012 from each observation in 1975 (blue) and 2006-2012 (red), and from each grid point of each CESM1 (black) and CESM2 (purple) simulation of 1975 and 2006-2012. Solid dots and lines indicate mean and one standard deviation.

143 simulate a 1970-2020 surface layer that is more consistent with observations in 1975 than  
 144 in 2006-2012 (comparing Fig. 2a with Figs. 2b-c).

145 Focusing on August (the lowest monthly salinity in the models; Fig. 2d-e; Table S2),  
 146 we find that CESM1 indicates a 2006-2012 August surface layer that is only  $0.7 \pm 1.0$  g/kg  
 147 fresher than in 1975, similar to CESM2 ( $0.6 \pm 0.9$  g/kg). By contrast, the observations  
 148 indicate an average  $3.6 \pm 1.0$  g/kg change toward a fresher surface layer during the same  
 149 time periods. As a consequence, we find that models are consistent with observations  
 150 in 1975 but not in 2006-2012. From all simulations, only 1.4% of CESM1 grid cells and  
 151 only 0.3% of CESM2 grid cells have a surface salinity that is as salty as any observation.  
 152 We find similar results for other months (Fig. S1-S2).

153 Overall, Figures 1-2 show that the models do not simulate the 1975 to 2006-2012  
 154 surface salinity change observed in the Canada Basin and that this bias cannot be ex-  
 155 plained by regional or internal variability present within the models. In the remainder  
 156 of this section, we consider three factors related to seasonal surface processes to iden-  
 157 tify sources of the surface freshening model bias.

### 158 3.2 Seasonal freshwater storage

159 We first examine the total amount of freshwater stored seasonally in the upper-ocean  
 160 by comparing the seasonal evolution of the observed and simulated salinity profiles. Specif-  
 161 ically, we use the upper-ocean seasonal freshwater content relative to May-average con-  
 162 ditions (sFWC), given by:

$$\text{sFWC}(t) = \int_{Z_{fw}(t)}^0 \frac{S_{\text{May}} - S(t, z)}{S_{\text{May}}} \cdot dz, \quad (1)$$

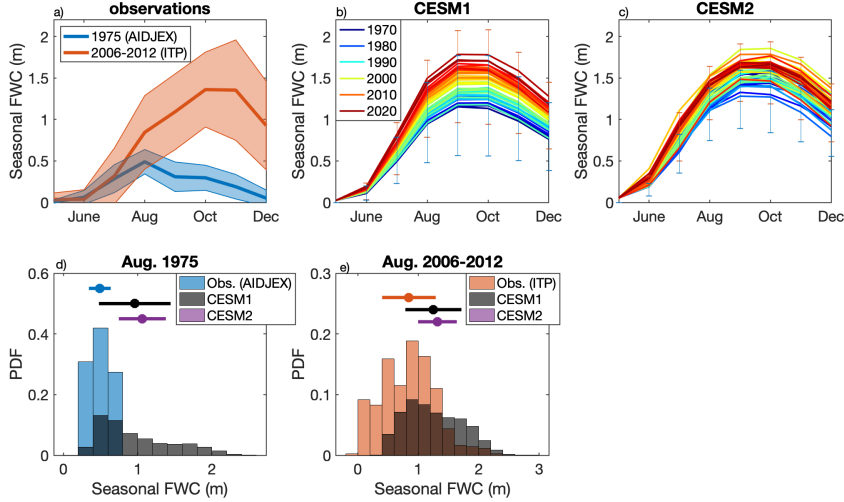


**Figure 3.** (a) Observed sFWC from 1975 AIDJEX data (blue) and 2006-2012 ITP data (red). Solid line indicates monthly-mean and shading indicates one standard deviation. (b-c) Simulated 1970-2020 ensemble-mean sFWC from (b) CESM1 and (c) CESM2. Blue and red error bars indicate one standard deviation over all grid points and simulations in 1975 and 2006-2012, respectively. (d-e) Distribution of August sFWC in (d) 1975 and (e) 2006-2012 from each observation in 1975 (blue) and 2006-2012 (red), and from each grid point of each CESM1 (black) and CESM2 (purple) simulation of 1975 and 2006-2012. Solid dots and lines indicate mean and one standard deviation.

163 where  $S$  is salinity, and  $Z_{fw}$  indicates the vertical extent of mixing defined by  $S(Z_{fw}) =$   
 164  $S_{May}$ , where  $z$  and  $Z_{fw}$  are both negative.  $S_{May}$  is the May-average surface salinity, which  
 165 is computed separately for each grid box of each year in each model simulation and is  
 166 computed separately for each ITP or AIDJEX ice camp of each year in the observations.  
 167 We compute sFWC from May-December at each grid point in each simulation of 1970-  
 168 2020 from each model and for each observation in 1975 and 2006-2012 (Fig. 3).

169 The value sFWC represents the amount of freshwater necessary to explain the tran-  
 170 sition from a well-mixed May salinity profile ( $S_{May}$ ) to any subsequent profile ( $S(t, z)$ )  
 171 for  $z \geq Z_{fw}$  at a given location in the models or observations. That is, sFWC indicates  
 172 the amount of freshwater contained in seasonal halocline, which reflects any process that  
 173 drives changes to the upper-ocean salinity, including sea ice melt, river runoff, precip-  
 174 itation, or advection. Figure S3 shows examples of this calculation from single profiles.

175 The expression for sFWC differs from the more often used expression for freshwa-  
 176 ter content in which the reference salinity is set to 34.8 g/kg. Instead, we use a refer-  
 177 ence salinity that is set to the May-average surface salinity. This difference implies that  
 178 sFWC reflects the seasonal near-surface freshwater content over a well-defined volume  
 179 (see SI for full derivation of sFWC), which avoids errors that can arise when using an  
 180 arbitrary reference salinity (Schauer & Losch, 2019). Furthermore, we use the same cri-  
 181 terion for  $S_{May}$  in both the models and observations, allowing for a fair comparison.

182 In both models and observations, we find that the average sFWC increases through  
 183 the summer and into the fall, coinciding with the summer melt season, river runoff, and  
 184 the intensification of the convergent Beaufort Gyre circulation. In late fall and early win-  
 185 ter, both the models and observations indicate an average decrease of sFWC, coincid-

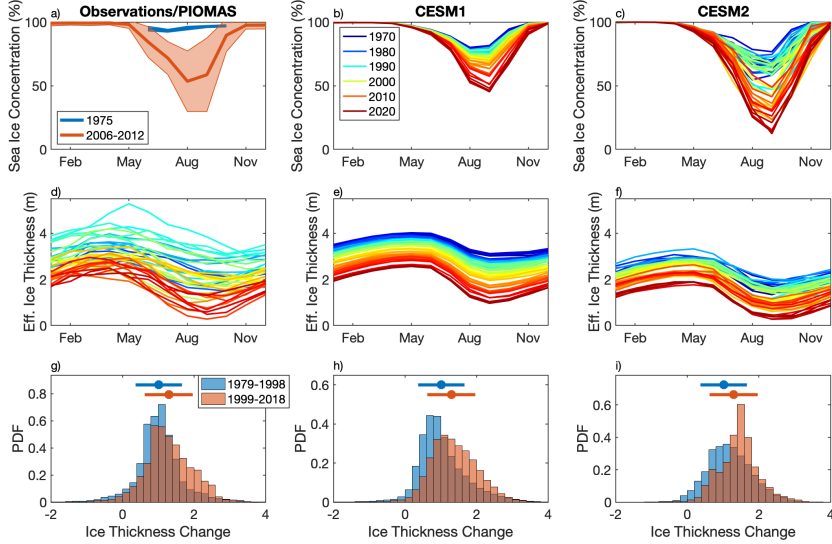


**Figure 4.** (a) Observed sea ice concentration co-located to 1975 AIDJEX data (blue) and 2006-2012 ITP data (red). Solid line indicates monthly mean and shading indicates standard deviation. (b-c) Simulated 1970-2020 ensemble-mean sea ice concentration from (b) CESM1 and (c) CESM2. (d-f) Effective sea ice thickness from (d) PIOMAS and (e,f) CESM1,2 ensemble mean. (g-i) Distribution of the seasonal change of the effective sea ice thickness between May and September during 1979-1998 (blue) and 1999-2018 (red) using all grid points from (g) PIOMAS, and from each (h) CESM1 and (i) CESM2 simulation. Solid dots and lines indicate the mean and standard deviation.

186 ing with brine rejection from freeze-up. As in Section 3.1, we consider the distribution  
 187 of the sFWC from every observation and from every grid point of every simulation in  
 188 August 1975 and 2006-2012 (Fig. 3d-e). We find that, on average, the August sFWC is  
 189 0.2-0.4 m larger in the models than in the observations during both time periods (Ta-  
 190 ble S2). We find similar results for other months, with the bias decreasing in fall 2006-  
 191 2012 and increasing in fall 1975 (Fig. 3a-c;S4-S5), suggesting a bias related to the Ek-  
 192 man convergence of freshwater in 1975. Together, this causes a smaller change in sFWC  
 193 between 2006-2012 and 1975 in the models than in the observations.

194 Overall, we find that the models appear to simulate at least as much freshwater  
 195 stored near the surface on seasonal timescales as the observations. This suggests that  
 196 insufficient seasonal freshwater input at the surface is not the likely source of the sur-  
 197 face freshening model bias (Figs. 1-2).

### 198 3.3 Sea ice conditions

199 Seasonal changes to the Arctic Ocean surface layer are primarily driven by the sea-  
 200 sonal melting and freezing of sea ice (McPhee & Smith, 1976; Morison & Smith, 1981;  
 201 Lemke & Manley, 1984; Peralta-Ferriz & Woodgate, 2015). In the models, the observa-  
 202 tions, and PIOMAS, we find a clear seasonal cycle and a considerable decline in both  
 203 summer sea ice concentration (Fig. 4a-c) and effective sea ice thickness (Fig. 4d-f). To  
 204 examine the decadal changes in seasonal sea ice volume evolution, which directly impacts  
 205 the seasonal freshwater surface flux, we compute a seasonal change (September - May)

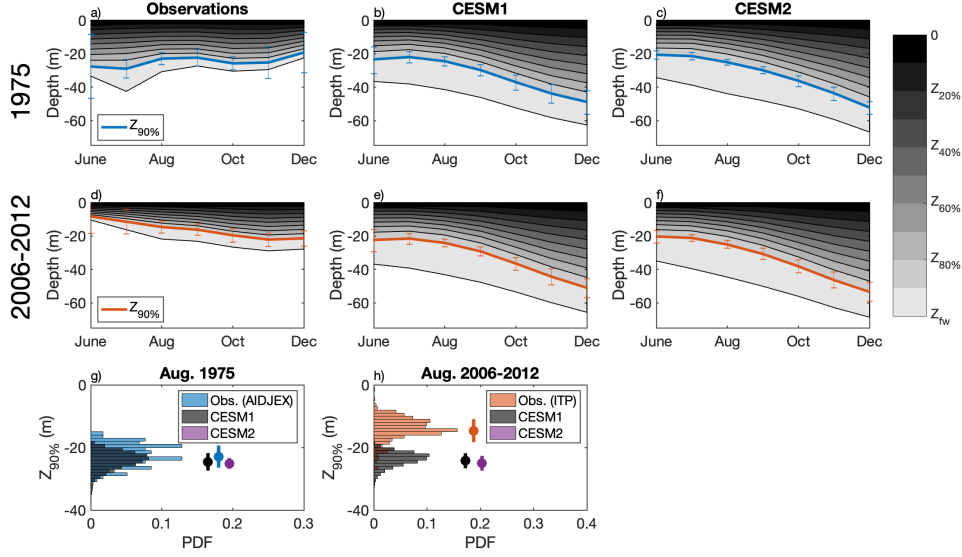


**Figure 5.** (a-f) Black solid lines separating each gray shading indicate the monthly-average depths of  $Z_{10\%}, Z_{20\%}, \dots, Z_{May}$  (eq. 2) from (a,d) observations, (b,e) CESM1 ensemble-mean, and (c,f) CESM2 ensemble mean in (a-c) 1975 and (d-f) 2006-2012. Dashed lines indicate  $Z_{90\%}$  in 1975 (a-c, blue) and 2006-2012 (d-f, red). Blue and red error bars indicate one standard deviation over all grid points and simulations in 1975 and 2006-2012, respectively. (g-h) Distribution of August  $Z_{90\%}$  in (g) 1975 and (h) 2006-2012 from each observation 1975 (blue) and 2006-2012 (red), and from each grid point of each CESM1 (black) and CESM2 (purple) simulation of 1975 and 2006-2012. Solid dots and lines indicate mean and one standard deviation.

206 in the effective ice thickness in each grid box in PIOMAS and in each simulation of CESM1  
 207 and CESM2 during 1979-2018 (Fig. 4g-i).

208 On average, PIOMAS, CESM1, and CESM2 indicate similar seasonal sea ice thick-  
 209 ness changes during the melt season in 1979-1998 ( $0.9 \pm 0.6$  m,  $0.8 \pm 0.6$  m, and  $1.0 \pm 0.5$  m,  
 210 respectively) and in 1999-2018 ( $1.1 \pm 0.6$  m,  $1.1 \pm 0.6$  m, and  $1.3 \pm 0.5$  m, respectively). These  
 211 results suggest that CESM1 and CESM2 are able to realistically simulate the seasonal  
 212 sea ice volume evolution in the Canada Basin, consistent with previous studies (see Meth-  
 213 ods). This suggests that, while there are differences in sea ice concentration between the mod-  
 214 els and observations (Fig. 4a-c; Table S2), seasonal sea ice volume biases are unlikely  
 215 to explain the surface freshening model bias (Fig. 1-2).

### 216 3.4 Vertical freshwater distribution

217 Finally, we compare the vertical distribution of the seasonal freshwater storage in  
 218 the models and observations, which we quantify by rewriting the expression for sFWC  
 219 as:

$$\begin{aligned}
 \text{sFWC} = & \underbrace{\int_{Z_{10\%}}^0 \frac{S_{\text{May}} - S(z)}{S_{\text{May}}} \cdot dz}_{=10\% \text{ of sFWC}} + \underbrace{\int_{Z_{20\%}}^{Z_{10\%}} \frac{S_{\text{May}} - S(z)}{S_{\text{May}}} \cdot dz}_{=10\% \text{ of sFWC}} + \dots + \underbrace{\int_{Z_{fw}}^{Z_{90\%}} \frac{S_{\text{May}} - S(z)}{S_{\text{May}}} \cdot dz}_{=10\% \text{ of sFWC}}, \\
 & \hspace{15em} (2)
 \end{aligned}$$

220 where  $Z_{10\%}, Z_{20\%}, \dots, Z_{f_w}$  is the lower bound of the depth range that encompasses 10%,  
 221 20%, ..., 100% of the sFWC. These depths are computed at each grid point of each sim-  
 222 ulation and each observation during May-December of 1975 and 2006-2012 (Figure 5).  
 223 We only include data points with positive values of sFWC, implying that some observed  
 224 June profiles are not included in this portion of the analysis. As in Section 3.3, we also  
 225 consider the August distribution of the  $Z_{90\%}$  from every observation and from every grid  
 226 point of every simulation in 1975 and 2006-2012 (5g-i; Table S2). We note that  $Z_{90\%}$  is  
 227 closely related to the mixed-layer depth in both the models and observations (Fig. S6).

228 The vertical distribution of sFWC reveals two discrepancies between the models  
 229 and observations (Fig. 5). First, we find that the freshwater is spread over a deeper range  
 230 in the simulations (Aug.  $Z_{90\%} = 24 \pm 2.7$  m,  $25 \pm 2.4$  m in CESM1, CESM2) compared  
 231 to the observations (Aug.  $Z_{90\%} = 14 \pm 3.7$  m) in 2006-2012. Second, we find that the ver-  
 232 tical distribution of sFWC remains relatively unchanged between 1975 and 2006-2012  
 233 in the simulations ( $\sim 0.1$  m change in Aug.  $Z_{90\%}$ ), while the observations indicate that  
 234 the freshwater is concentrated significantly closer to the surface in 2006-2012 than in 1975  
 235 ( $\sim 8$  m change). Interestingly, we find that the models do simulate a 1975 vertical dis-  
 236 tribution of sFWC consistent with the observations during the summer (Aug.  $Z_{90\%} = 23 \pm 3.5$  m,  
 237  $25 \pm 2.8$  m, and  $26 \pm 1.7$  m in the observations, CESM1, and CESM2, respectively), sim-  
 238 ilar to the 1975 surface salinity (Fig. 2).

239 Overall, we find that the 2006-2012 seasonal freshwater storage has an unrealistic  
 240 vertical distribution in the models, and that the discrepancy between the models and  
 241 observations cannot be explained by regional or internal variability present within the  
 242 models (Fig. 5g-h). Together this suggests that simulated vertical mixing of freshwater  
 243 is inconsistent with observations in recent years and that this is a likely source of the sur-  
 244 face freshening model bias (Fig. 1,2).

## 245 4 Conclusions

246 State-of-the-art coupled ice-ocean models struggle to accurately simulate upper-  
 247 ocean stratification in the Canada Basin, and instead tend to simulate a surface layer  
 248 that is saltier and less stratified than observed (Holloway et al., 2007; Ilicak et al., 2016).  
 249 The bias could be related to sea ice, atmospheric, or ocean processes and, until now, had  
 250 only been examined using numerical experiments and annual climatologies (Holloway et  
 251 al., 2007; Ilicak et al., 2016; Nguyen et al., 2009; Zhang & Steele, 2007; Jin et al., 2012;  
 252 Barthélemy et al., 2015; Sidorenko et al., 2018).

253 Here, we examine this question by focusing on decadal changes to seasonal surface  
 254 processes using observations from below-ice ocean measurements collected during May-  
 255 December 1975 (AIDJEX) and 2006-2012 (ITPs) and in the two most recent generations  
 256 of the Community Earth Systems Models (CESM1 and CESM2). We find that CESM  
 257 simulates upper-ocean salinities that are fairly consistent with the observations in 1975,  
 258 but it fails to capture the fresh surface layer that appears in the 2006-2012 observations  
 259 (Figs. 1-2). We show that the surface freshening model bias is likely related to the un-  
 260 realistically deep mixing of freshwater in the models (Fig. 5), rather than insufficient fresh-  
 261 water input from sea ice melt or other sources (Fig. 3 - 4). Overall, the results show that  
 262 CESM1 and CESM2 simulate a mixed layer that is too salty and deep, similar to most  
 263 ice-ocean models (Ilicak et al., 2016), and are not able to simulate the observed reduc-  
 264 tion in mixed-layer depth associated with increased surface freshwater fluxes. Moreover,  
 265 CESM systematically simulates a mixed-layer depth consistent with observations in 1975  
 266 and a seasonal freshwater input that is similar to observations in 2006-2012. This sug-  
 267 gests that one source of the 2006-2012 ocean stratification bias is related to missing or  
 268 unrealistic summer mixed-layer dynamics in recent years, rather than sea ice or atmo-  
 269 spheric processes, possibly due to unrealistically high vertical mixing or low vertical res-  
 270 olution in the models.

271 These results raise important questions related to the ramifications of this bias on  
 272 Arctic ecosystem dynamics and on the sea ice cover because the upper-ocean stratifica-  
 273 tion directly impacts the vertical exchange of heat, energy, and nutrients. For example,  
 274 if the unrealistically deep transport of freshwater carries heat downwards and traps nu-  
 275 trients deeper, then there would be less heat available for summer sea ice melt, a weaker  
 276 seasonal ice-albedo feedback, and reduced primary productivity. These results, there-  
 277 fore, highlight the need for improved parameterizations of upper-ocean dynamics under  
 278 a rapidly changing sea ice cover.

## 279 Acknowledgments

280 The AIDJEX data used in this study can be found at <http://lwbin-datahub.ad.umanitoba.ca/dataset/aidjex>.  
 281 The Ice-Tethered Profiler data were collected and made available by the Ice-Tethered  
 282 Profiler Program based at the Woods Hole Oceanographic Institution (<http://www.whoi.edu/itp>).  
 283 All sea ice concentration data created or used during this study are openly available from  
 284 the NASA National Snow and Ice Data Center Distributed Active Archive Center at <https://doi.org/10.5067/8GC>  
 285 as cited in Cavalieri1996.

286 ER was supported by the National Sciences and Engineering Research Council of  
 287 Canada (NSERC) PDF award. ER and JS were supported by the NSERC Canada-150  
 288 Chair. STG was supported by the US NSF (Awards PLR-1425989 and OPP-1936222)  
 289 and by the US Department of Energy (DOE) (Award DE-SC0020073). This work is a  
 290 contribution to the NSERC - Discovery Grant and the NSF Office of Polar Program grant  
 291 # 1504023 awarded to LBT. RG was supported by the NSERC Canada Discovery Grant  
 292 program. RF acknowledges funding from NSERC Canada through a CGS-D award and  
 293 the US DOE (Grant DE-SC001940).

## 294 References

- 295 Barthélemy, A., Fichet, T., Goosse, H., & Madec, G. (2015). Modeling the inter-  
 296 play between sea ice formation and the oceanic mixed layer: Limitations of  
 297 simple brine rejection parameterizations. *Ocean Modelling*, *86*, 141–152. doi:  
 298 10.1016/j.ocemod.2014.12.009
- 299 Brown, K. A., Holding, J. M., & Carmack, E. C. (2020). Understanding Regional  
 300 and Seasonal Variability is key to Gaining a Pan-Arctic Perspective on Arctic  
 301 Ocean Freshening. *Frontiers Mar. Sci*, *7*, 606. doi: 10.3389/fmars.2020.00606
- 302 Carmack, E., Polyakov, I., Padman, L., Fer, I., Hunke, E., Hutchings, J., . . . Winsor,  
 303 P. (2015). Towards Quantifying the Increasing Role of Oceanic Heat in Sea Ice  
 304 Loss in the New Arctic. *Bulletin of the American Meteorological Society*. doi:  
 305 10.1175/BAMS-D-13-00177.1
- 306 Carmack, E. C., Yamamoto-Kawai, M., Haine, T. W. N., Bacon, S., Bluhm, B. A.,  
 307 Lique, C., . . . Williams, W. J. (2016). Freshwater and its role in the Arctic  
 308 Marine System: Sources, disposition, storage, export, and physical and biogeo-  
 309 chemical consequences in the Arctic and global oceans. *Journal of Geophysical*  
 310 *Research: Biogeosciences*, *121*, 675–717. doi: 10.1002/2015JG003140
- 311 Cavalieri, D., Parkinson, C. L., Gloersen, P., & Zwally, H. J. (1996). Sea Ice Con-  
 312 centrations from SMMR and DMSP SSM/I-I-SSMIS Passive Microwave Data,  
 313 Version1. *Natl. Snow and Ice Data Cent., Boulder, Colo.* ((Updated 2015.)  
 314 <https://nsidc.org/data/nsidc-0051>)
- 315 Danabasoglu, G., Lamarque, J. F., Bacmeister, J., Bailey, D. A., DuVivier, A. K.,  
 316 Edwards, J., . . . Strand, W. G. (2020). The Community Earth System Model  
 317 Version 2 (CESM2). *Journal of Advances in Modeling Earth Systems*, *12*(2),  
 318 1–35. doi: 10.1029/2019MS001916
- 319 Holloway, G., Dupont, F., Golubeva, E., Häkkinen, S., Hunke, E., Jin, M., . . .  
 320 Zhang, J. (2007). Water properties and circulation in Arctic Ocean  
 321 models. *Journal of Geophysical Research: Oceans*, *112*(4), 1–18. doi:

- 10.1029/2006JC003642
- 322 Ilicak, M., Drange, H., Wang, Q., Gerdes, R., Aksenov, Y., Bailey, D., . . . Yeager,  
323 S. G. (2016). An assessment of the Arctic Ocean in a suite of interannual  
324 CORE-II simulations. Part III: Hydrography and fluxes. *Ocean Modelling*,  
325 *100*, 141–161.
- 326 Jackson, J. M., Allen, S. E., McLaughlin, F. A., Woodgate, R. A., & Carmack,  
327 E. C. (2011). Changes to the near-surface waters in the Canada Basin, Arctic  
328 Ocean from 1993-2009: A basin in transition. *Journal of Geophysical Research:*  
329 *Oceans*, *116*, 1–21. doi: 10.1029/2011JC007069
- 330 Jackson, J. M., Carmack, E. C., McLaughlin, F. A., Allen, S. E., & Ingram, R. G.  
331 (2010). Identification, characterization, and change of the near-surface tem-  
332 perature maximum in the Canada Basin, 1993-2008. *Journal of Geophysical*  
333 *Research: Oceans*, *115*, 1–16. doi: 10.1029/2009JC005265
- 334 Jackson, J. M., Williams, W. J., & Carmack, E. C. (2012). Winter sea-ice melt in  
335 the Canada Basin, Arctic ocean. *Geophysical Research Letters*, *39*, 2–7. doi:  
336 10.1029/2011GL050219
- 337 Jin, M., Hutchings, J., Kawaguchi, Y., & Kikuchi, T. (2012). Ocean mixing  
338 with lead-dependent subgrid scale brine rejection parameterization in a cli-  
339 mate model. *Journal of Ocean University of China*, *11*(4), 473–480. doi:  
340 10.1007/s11802-012-2094-4
- 341 Kay, J. E., Deser, C., Phillips, A., Mai, A., Hannay, C., Strand, G., . . . Vertenstein,  
342 M. (2015). The community earth system model (CESM) large ensemble  
343 project : A community resource for studying climate change in the presence of  
344 internal climate variability. *Bulletin of the American Meteorological Society*,  
345 *96*, 1333–1349. doi: 10.1175/BAMS-D-13-00255.1
- 346 Krishfield, R., Toole, J., Proshutinsky, A., & Timmermans, M. L. (2008). Auto-  
347 mated ice-tethered profilers for seawater observations under pack ice in all  
348 seasons. *Journal of Atmospheric and Oceanic Technology*, *25*(11), 2091–2105.  
349 doi: 10.1175/2008JTECHO587.1
- 350 Labe, Z., Magnusdottir, G., & Stern, H. (2018). Variability of Arctic sea ice thick-  
351 ness using PIOMAS and the CESM large ensemble. *Journal of Climate*, *31*(8),  
352 3233–3247. doi: 10.1175/JCLI-D-17-0436.1
- 353 Large, W. G., McWilliams, J. C., & Doney, S. C. (1994). Oceanic vertical mixing: A  
354 review and a model with a nonlocal boundary layer parameterization. *Reviews*  
355 *of Geophysics*, *34*(4), 363–403. doi: 10.1029/94RG01872
- 356 Lemke, P., & Manley, T. O. (1984). The seasonal variation of the mixed layer and  
357 the pycnocline under polar sea ice. *Journal of Geophysical Research*, *89*, 6494.  
358 doi: 10.1029/JC089iC04p06494
- 359 McLaughlin, F., Carmack, E., Proshutinsky, A., Krishfield, R., Guay, C., Yamamoto-  
360 Kawai, M., . . . Williams, B. (2011). The Rapid Response of the Canada  
361 Basin to Climate Forcing. *Oceanography*, *24*, 136–145. doi: 10.5670/  
362 oceanog.2011.66
- 363 McLaughlin, F. A., & Carmack, E. C. (2010). Deepening of the nutricline and  
364 chlorophyll maximum in the Canada Basin interior, 2003-2009. *Geophysical*  
365 *Research Letters*, *37*(24), 1–5. doi: 10.1029/2010GL045459
- 366 McPhee, M. G., & Smith, J. D. (1976). Measurements of the turbulent boundary  
367 layer under pack ice. *Journal of Physical Oceanography*, *6*, 696–711. doi: 10  
368 .1175/1520-0485(1976)006(0696:MOTTBL)2.0.CO;2
- 369 Morison, J., & Smith, J. D. (1981). Seasonal variations in the upper Arctic Ocean  
370 as observed at T-3. *Geophysical Research Letters*, *8*, 753–756. doi: 10.1029/  
371 GL008i007p00753
- 372 Nguyen, A. T., Menemenlis, D., & Kwok, R. (2009). Improved modeling of the arctic  
373 halocline with a subgrid-scale brine rejection parameterization. *Journal of*  
374 *Geophysical Research: Oceans*, *114*(11), 1–12. doi: 10.1029/2008JC005121
- 375 Peralta-Ferriz, C., & Woodgate, R. A. (2015). Seasonal and interannual vari-  
376

- 377 ability of pan-Arctic surface mixed layer properties from 1979 to 2012  
 378 from hydrographic data, and the dominance of stratification for multiyear  
 379 mixed layer depth shoaling. *Progress in Oceanography*, *134*, 19–53. doi:  
 380 10.1016/j.pocan.2014.12.005
- 381 Proshutinsky, A., Krishfield, R., Timmermans, M.-L., Toole, J., Carmack, E.,  
 382 McLaughlin, F., . . . Shimada, K. (2009). Beaufort Gyre freshwater reser-  
 383 voir: State and variability from observations. *Journal of Geophysical Research*,  
 384 *114*. doi: 10.1029/2008JC005104
- 385 Rosenblum, E., & Eisenman, I. (2016). Faster Arctic sea ice retreat in CMIP5 than  
 386 in CMIP3 due to volcanoes. *Journal of Climate*, *29*(24), 9179–9188. doi: 10  
 387 .1175/JCLI-D-16-0391.1
- 388 Rosenblum, E., & Eisenman, I. (2017). Sea ice trends in climate models only ac-  
 389 curate in runs with biased global warming. *Journal of Climate*, *30*(16), 6265–  
 390 6278. doi: 10.1175/JCLI-D-16-0455.1
- 391 Rosenblum, E., Stroeve, J. S., Gille, S., Tremblay, L., Carmack, E. C., Barber,  
 392 D. G., . . . Fajber, R. (2021). Freshwater input and vertical distribution  
 393 in the Canada Basin’s seasonal halocline: 1975 versus 2006–2012. *Preprint*:  
 394 <https://doi.org/10.1002/essoar.10507192.1>.
- 395 Schauer, U., & Losch, M. (2019). Freshwater in the ocean is not a useful parameter  
 396 in climate research. *Journal of Physical Oceanography*, *49*(9), 2309–2321. doi:  
 397 10.1175/JPO-D-19-0102.1
- 398 Schweiger, A., Lindsay, R., Zhang, J., Steele, M., & Stern, H. (2011). Uncertainty in  
 399 modeled Arctic sea ice volume. *Journal of Geophysical Research*.
- 400 Sidorenko, D., Koldunov, N. V., Wang, Q., Danilov, S., Goessling, H. F., Gurses, O.,  
 401 . . . Jung, T. (2018). Influence of a Salt Plume Parameterization in a Cou-  
 402 pled Climate Model. *Journal of Advances in Modeling Earth Systems*, *10*(9),  
 403 2357–2373. doi: 10.1029/2018MS001291
- 404 SIMIP. (2020). Arctic Sea Ice in CMIP6. *Geophysical Research Letters*, *47*(10). doi:  
 405 10.1029/2019gl086749
- 406 Steele, M., Ermold, W., & Zhang, J. (2011). Modeling the formation and  
 407 fate of the near-surface temperature maximum in the Canadian Basin of  
 408 the Arctic Ocean. *Journal of Geophysical Research*, *116*, C11015. doi:  
 409 10.1029/2010JC006803
- 410 Stroeve, J., Barrett, A., Serreze, M., & Schweiger, A. (2014). Using records  
 411 from submarine, aircraft and satellites to evaluate climate model simu-  
 412 lations of Arctic sea ice thickness. *Cryosphere*, *8*(5), 1839–1854. doi:  
 413 10.5194/tc-8-1839-2014
- 414 Stroeve, J., Holland, M. M., Meier, W., Scambos, T., & Serreze, M. (2007). Arctic  
 415 sea ice decline: Faster than forecast. *Geophysical Research Letters*, *34*, L09501.  
 416 doi: 10.1029/2007GL029703
- 417 Stroeve, J., Kattsov, V., Barrett, A., Serreze, M., Pavlova, T., Holland, M.,  
 418 & Meier, W. N. (2012). Trends in Arctic sea ice extent from CMIP5,  
 419 CMIP3 and observations. *Geophysical Research Letters*, *39*, L16502. doi:  
 420 10.1029/2012GL052676
- 421 Timmermans, M., & Marshall, J. (2020). Understanding Arctic Ocean Circulation:  
 422 A Review of Ocean Dynamics in a Changing Climate. *Journal of Geophysical*  
 423 *Research: Oceans*, *125*, 1–35. doi: 10.1029/2018jc014378
- 424 Timmermans, M. L. (2015). The impact of stored solar heat on Arctic sea  
 425 ice growth. *Geophysical Research Letters*, *42*, 6399–6406. doi: 10.1002/  
 426 2015GL064541
- 427 Tivy, A., Howell, S. E., Alt, B., McCourt, S., Chagnon, R., Crocker, G., . . . Yackel,  
 428 J. J. (2011). Trends and variability in summer sea ice cover in the Cana-  
 429 dian Arctic based on the Canadian Ice Service Digital Archive, 1960–2008  
 430 and 1968–2008. *Journal of Geophysical Research: Oceans*, *116*. doi:  
 431 10.1029/2009JC005855

- 432 Toole, J. M., Timmermans, M. L., Perovich, D. K., Krishfield, R. A., Proshutin-  
433 sky, A., & Richter-Menge, J. A. (2010). Influences of the ocean surface  
434 mixed layer and thermohaline stratification on Arctic Sea ice in the central  
435 Canada Basin. *Journal of Geophysical Research: Oceans*, *115*, 1–14. doi:  
436 10.1029/2009JC005660
- 437 Untersteiner, N., Thorndike, A. S., Rothrock, D. A., & Hunkins, K. L. (2007). AID-  
438 JEX revisited: A look back at the U.S.-Canadian Arctic Ice Dynamics Joint  
439 Experiment 1970-78. *Arctic*, *60*, 327–336. doi: 10.14430/arctic233
- 440 Wang, Q., Wekerle, C., Danilov, S., Koldunov, N., Sidorenko, D., Sein, D., . . . Jung,  
441 T. (2018). Arctic sea ice decline significantly contributed to the unprecedented  
442 liquid freshwater accumulation in the Beaufort Gyre of the Arctic Ocean. *Geo-*  
443 *physical Research Letters*, *45*(10), 4956–4964. doi: 10.1029/2018GL077901
- 444 Winton, M. (2011). Do climate models underestimate the sensitivity of northern  
445 hemisphere sea ice cover? *Journal of Climate*, *24*, 3924–3934. doi: 10.1175/  
446 2011JCLI4146.1
- 447 Yamamoto-Kawai, M., McLaughlin, F. A., Carmack, E. C., Nishino, S., Shimada,  
448 K., & Kurita, N. (2009). Surface freshening of the Canada Basin, 2003-  
449 2007: River runoff versus sea ice meltwater. *Journal of Geophysical Research:*  
450 *Oceans*, *114*, 2003–2007. doi: 10.1029/2008JC005000
- 451 Zhang, J., & Steele, M. (2007). Effect of vertical mixing on the Atlantic Water layer  
452 circulation in the Arctic Ocean. *Journal of Geophysical Research: Oceans*,  
453 *112*(4), 1–9. doi: 10.1029/2006JC003732